Chemical Geology 654 (2024) 122059

Contents lists available at ScienceDirect

Chemical Geology

journal homepage: www.elsevier.com/locate/chemgeo

Triple oxygen isotope systematics of CO_2 hydroxylation

David Bajnai [a,*], Xiaobin Cao [b], Swea Klipsch [c], Andreas Pack [a], Daniel Herwartz [c,d]

[a] Geoscience Center, University of Göttingen, Germany
[b] International Center for Isotope Effects Research, Nanjing University, China
[c] Institute for Geology and Mineralogy, University of Cologne, Germany
[d] Institute for Geology, Mineralogy and Geophysics, Ruhr University Bochum, Germany

ARTICLE INFO

Editor: Oleg Pokrovsky

Keywords:
Triple oxygen isotopes
CO_2 hydroxylation
CO_2 absorption
Kinetic isotope effect
Hydroxide ion
Carbonate
Water

ABSTRACT

Kinetic isotope effects occurring during carbonate precipitation impact the accuracy of paleoclimate records. One rate-limiting process is CO_2 absorption, which, at high pH, primarily proceeds through hydroxylation, where aqueous CO_2 and OH^- react to form HCO_3^-. In this study, we investigated the triple oxygen isotope fractionation ($^{18}O/^{16}O$ and $^{17}O/^{16}O$) associated with the hydroxylation reaction. We experimentally determined the extent of the kinetic isotope effects superimposed on the reacting CO_2 and OH^- during hydroxylation, using high-pH precipitation reactions. These results were compared to the equilibrium triple oxygen isotope fractionation between H_2O and OH^- modeled using quantum chemical computations.

Our quantum chemical modeling confirms the previously suggested equilibrium $\theta^{eq.}_{H2O/OH^-}$ of 0.5296 at 25 °C. Our empirical data show a kinetic isotope effect superimposed on the OH^- involved in the hydroxylation reaction of approximately −16.4‰ for the fractionation of $^{18}O/^{16}O$ and a corresponding slope of 0.514 in triple oxygen isotope space. The $\theta^{effective}_{H2O/OH^-}$ for the fractionation between water and the reacting OH^- is 0.523.

In order to identify and potentially correct kinetic isotope effects in carbonates, it is important to understand the fractionations occurring during precipitation. Our results enable a more accurate modeling of kinetic isotope effects in triple oxygen isotope space, particularly the slope of hydroxylation. The $\theta_{hydroxylation}$ is dependent on the isotope composition of the ambient water, CO_2, and the temperature. We estimate that $\theta_{hydroxylation}$ is approximately 0.532 for carbonates growing in 25 °C seawater.

1. Introduction

The oxygen isotope partitioning between minerals and water provides a temperature proxy, most prominently used for carbonates (Urey, 1947). At thermodynamic equilibrium, the oxygen isotope composition of a carbonate is only a function of precipitation temperature and the ambient water's isotopic composition. However, most carbonates do not form in full equilibrium due to, for example, the preferential reaction of light isotopologues during mineral growth (Daëron et al., 2019; Devriendt et al., 2017). This limits the usability of oxygen isotopes as a paleoclimate proxy.

The hydroxylation reaction, where dissolved CO_2 and OH^- react to form HCO_3^-, is one such source of disequilibrium:

$$CO_{2(aq)} + OH^-_{(aq)} \rightleftharpoons HCO^-_{3(aq)} \quad (1)$$

The isotopic composition of a bicarbonate produced via Eq. (1) is not in equilibrium with water, and neither is the carbonate that forms rapidly from the unequilibrated dissolved inorganic carbon (DIC) pool:

$$HCO_3^- \rightleftharpoons H^+ + CO_3^{2-} \quad (2)$$

$$Ba^{2+} + CO_3^{2-} \rightleftharpoons BaCO_3 \quad (3)$$

The "vital effects" observed in corals, brachiopods, and other marine calcifiers are partly related to the hydroxylation reaction and limit their usability as paleoclimate archives (e.g., Bajnai et al., 2018; Davies et al., 2023, 2022; McConnaughey, 1989a, 1989b).

The combined measurement of the three stable oxygen isotopes (^{16}O, ^{17}O, ^{18}O) adds another dimension to the traditional $\delta^{18}O$ scale, providing additional information on the fractionation processes and temperatures (Luz and Barkan, 2010; Pack and Herwartz, 2014). Triple oxygen isotopes can help to identify if carbonates were formed in equilibrium or through kinetic processes, an approach similar to using dual clumped isotopes (Bajnai et al., 2020). Samples in thermodynamic equilibrium will fall on the equilibrium curve in the triple oxygen

* Corresponding author.
E-mail address: david.bajnai@uni-goettingen.de (D. Bajnai).

https://doi.org/10.1016/j.chemgeo.2024.122059
Received 22 December 2023; Received in revised form 18 March 2024; Accepted 21 March 2024
Available online 23 March 2024

isotope, i.e., the δ'^{18}O vs. Δ'^{17}O space. In contrast, samples affected by individual kinetic processes will show an offset from the equilibrium curve (Guo and Zhou, 2019; Herwartz, 2021). Knowing the expected slope of the offset for a given kinetic process allows correcting for the kinetic part and deducing accurate paleotemperatures.

To predict the kinetic slope for the hydroxylation reaction in triple oxygen isotope space, it is necessary to know the triple oxygen isotopic composition of the reacting species, which are CO_2 and OH^-. Here, we focus on the triple oxygen isotopic composition of the ambient aqueous hydroxide ion (OH^-), which is constantly produced and consumed in any aqueous environment:

$$H_2O^{16} + O^iH^- \rightleftharpoons H_2O^i + O^{16}H^- \quad (4)$$

For Eq. (4), the isotope fractionation factor α is defined as:

$$\alpha^i_{H_2O/OH^-} = \frac{(\delta^i O_{H_2O} + 1)}{(\delta^i O_{OH^-} + 1)} \quad (5)$$

where i denotes a rare isotope substitution, i.e., ^{18}O and ^{17}O. In turn, the fractionation of ^{17}O/^{16}O relative to ^{18}O/^{16}O between H_2O and OH^-, is given by:

$$\theta_{H_2O/OH^-} = \frac{ln\left(\alpha^{17}_{H_2O/OH^-}\right)}{ln\left(\alpha^{18}_{H_2O/OH^-}\right)} \quad (6)$$

The θ of mass-dependent equilibrium fractionation processes generally falls between 0.52 and the theoretical limit of 0.5305 (Cao and Liu, 2011; Herwartz, 2021; Matsuhisa et al., 1978; Young et al., 2002). To better illustrate differences between different fractionation processes, the Δ'^{17}O value (here in ppm) is used:

$$\Delta'^{17}O = 10^6 \cdot ln\left(\frac{\delta^{17}O}{1000} + 1\right) - \lambda_{RL} \times 10^6 \cdot ln\left(\frac{\delta^{18}O}{1000} + 1\right) \quad (7)$$

We choose the slope of the meteoric water line, 0.528, for λ_{RL} (Luz and Barkan, 2010). The $10^3 ln(\delta^{17}O/10^3 + 1)$ and the $10^3 ln(\delta^{18}O/10^3 + 1)$ are termed "linearized form of the δ–notation"and reported as δ'^{17}O and δ'^{18}O, respectively (Hulston and Thode, 1965; Miller, 2002).

Only a few experimental studies have attempted to constrain the δ^{18}O of dissolved OH^- (Bajnai and Herwartz, 2021; Green and Taube, 1963), and respective data for Δ'$^{17}O_{OH-}$ are presently missing. Bajnai and Herwartz (2021) determined the $\delta^{18}O_{OH-}$ from the oxygen isotope composition of ambient water and carbonates from high-pH precipitation experiments. In their experimental setup, CO_2 absorption exclusively proceeded via hydroxylation. At pH > 12, hydroxylation is the rate-limiting reaction during carbonate precipitation (Eqs. (1)–(3)), at least within their experimental design, where fast net precipitation and high pH hinder significant isotope exchange between the DIC pool and water. They show that the reacting OH^- is depleted in δ^{18}O by about 15–20‰ relative to the OH^- in equilibrium with water. This is in agreement with the prediction by Zeebe (2020). We note here that Bajnai and Herwartz (2021) corrected their carbonate δ^{18}O data by −1.03‰ to account for the difference between the calcite and witherite acid fractionation factors. Because there is no witherite acid fractionation factor for ^{17}O/^{16}O, for consistency, we use only calcite-corrected data.

If CO_2 is quantitatively and rapidly precipitated as carbonate, the respective back-reactions in Eqs. (1)–(3), can be considered insignificant. Thus, the mineral inherits 2/3 of its oxygen from CO_2 and 1/3 from the hydroxide ion (e.g., Bajnai and Herwartz, 2021; Devriendt et al., 2017; Sade and Halevy, 2017). The near-quantitative consumption of CO_2 with known isotopic composition then allows calculating the isotope composition of the OH^- from carbonate analyses:

$$\delta^i O_{mineral} = \frac{2}{3}\delta^i O^{effective}_{CO_2} + \frac{1}{3}\delta^i O^{effective}_{OH^-} \quad (8)$$

It is crucial to emphasize that such experiments cannot be used to calculate equilibrium isotope fractionations because the reactants (OH^- and CO_2) include superimposed kinetic effect (KIE_{OH-} and KIE_{CO2}):

$$\delta^{effective} = \delta^{equilibrium} + KIE \quad (9)$$

Consequently, the experimentally determined effective oxygen isotope fractionation factors ($\alpha^{effective}_{H2O/OH-}$) are not representative of the thermodynamic equilibrium of Eq. (4) ($\alpha^{equilibrium}_{H2O/OH-}$) because of the superimposed KIE. In the experimental setup of Bajnai and Herwartz (2021) the magnitude of the KIE_{CO2} is close to zero because all injected CO_2 is nearly quantitatively consumed, yet the KIE_{OH-} is fully expressed. In this study, we report KIE as the natural logarithm of a fractionation factor, multiplied by one thousand.

The comprehensive numerical triple oxygen Isotope model of Guo and Zhou (2019) provides theoretical data for the CO_2 hydroxylation reaction in triple oxygen isotope space. However, in their calculations, these authors used the experimental equilibrium H_2O/OH^- oxygen isotope fractionation factor from Green and Taube (1963) combined with the theoretical temperature dependence following Hunt and Taube (1959). More recent theoretical modeling has called the accuracy of these early data into question (Zeebe, 2020), and this interpretation is corroborated by the results presented herein. Therefore, the estimates by Guo and Zhou (2019) for the kinetic isotope fractionation exerted by CO_2 hydroxylation may be inaccurate. Huth et al. (2022) explored speleothem growth, and their empirical slopes in triple oxygen isotope space do not follow the theoretical CO_2 degassing trajectories of Guo and Zhou (2019), either implying that other processes, such as evaporation, are more important than previously considered or that the theoretical CO_2 degassing slope is inaccurate. This example highlights the urgent need for combined experimental and theoretical studies to assess kinetics in the dissolved inorganic carbon (DIC)-H_2O-CO_2 system.

In this study, we estimate the equilibrium $\theta_{H2O/OH-}$ using ab initio quantum chemical calculations, and, using high-pH carbonate precipitation experiments, assess the KIE_{OH-} and KIE_{CO2} in triple oxygen isotope space. We further compare theoretical slopes for KIE_{OH-} with empirical estimates. The consistent results provide a robust estimate for the triple oxygen isotopic composition of the reacting OH^-. These results are significant beyond the field of carbonate geochemistry, as all reactions with water may also involve oxygen derived from OH^- or H_3O^+. The robust interpretation of respective oxygen isotope data requires knowledge of the isotopic composition of all reacting species.

2. Materials and methods

2.1. Precipitation experiments

To precipitate witherite ($BaCO_3$), CO_2 was rapidly reacted with a pH ≈ 13 barium-hydroxide solution (c.f., Bajnai and Herwartz, 2021). A total of eleven precipitation experiments were conducted for this study, designated as Exp. A–K. First, CO_2 gas ($\delta^{13}C$ = 4.6‰ VPDB, $\delta^{18}O$ = 32.5‰ VSMOW) was frozen into ¼" evacuated quartz tubes, which were then flame-sealed. In all experiments, the amount of the CO_2 was similar, approximately 10^{-4} mol, achieved by maintaining the pressure, temperature, and volume (i.e., length of the quartz tubes) constant. To prepare the barium-hydroxide solution, approximately 90 mg of $Ba(OH)_2 \times 8H_2O$ was dissolved in filtered (Milli-Q) tap water at room temperature, yielding a saturated (0.22 mol L^{-1}) solution. Excess salt and precipitates were filtered out from the solution under a CO_2-free nitrogen atmosphere. The solution was stored overnight before conducting the precipitation experiments.

The precipitation experiments were performed in a glove box and a CO_2-free nitrogen atmosphere at a temperature of 22(±1) °C (Fig. 1). The CO_2 break seal tubes were inserted into a larger, flexible PTFE tube (step 1). The remaining volume of the PTFE tube was completely filled with the barium-hydroxide solution, ensuring that no bubbles were visible after closing it (step 2). Approximately 12 mL of the solution was

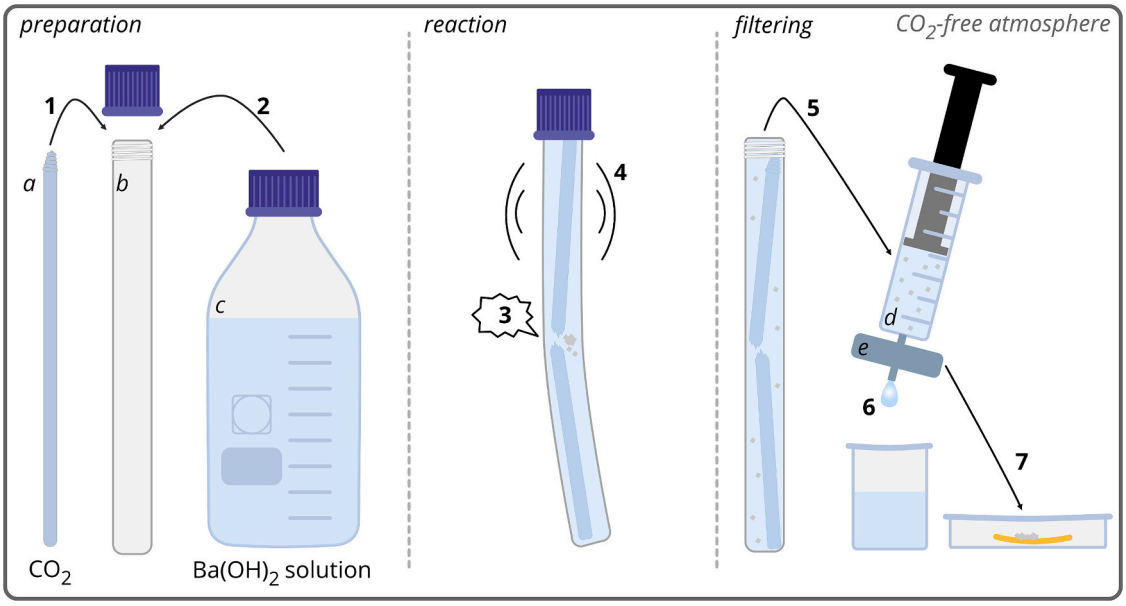

Fig. 1. Overview of the carbonate precipitation procedure. The numbered arrows depict the seven experimental steps as explained in the text. A: flame-sealed tube with CO_2 inside, b: PTFE tube with air-tight screw-top, c: barium-hydroxide solution, d: glass syringe, e: filter holder.

used, which was more than the amount required to react with all the CO_2 (approximately 0.4 mL). By bending the PTFE tube, the break seal tube was cracked inside, initiating the precipitation of $BaCO_3$ (step 3). Briefly shaking the vial helped the CO_2 gas escape from the break seal tube and disperse the bubbles (step 4). Finally, the solution was siphoned into a glass syringe (step 5) and passed through a stainless-steel syringe filter holder (Whatman FM025/0) with a 25-mm-diameter and 0.45-μm-pore cellulose acetate filter paper (step 6). The precipitate was rinsed with an ample amount of purified water before removing the filter paper from its holder. Lastly, the precipitate was left to dry overnight on the filter paper within the glove box (step 7).

Each experiment except for Exp. J yielded 17–23 mg of witherite, which corresponds to a near 100% yield (expected 18–19 mg; Table S1). In contrast, Exp. J only produced 10 mg of carbonate, resulting in a calculated yield of approximately 50%.

2.2. Isotope analyses of CO_2 and witherite

For this study, we analyzed the triple oxygen and carbon isotope composition ($\delta^{18}O$ and $\Delta'^{17}O$) of witherite precipitates, as well as the CO_2 and the solution used for the precipitation experiments. We report all oxygen isotope values relative to VSMOW and carbon isotope values relative to VPDB.

Five out of the eleven precipitates were analyzed for triple oxygen isotopes. Carbonate samples were digested in 103% phosphoric acid at 25 °C. Approximately 4 mg of $BaCO_3$ (around 2 mg of $CaCO_3$ for the calcite standards) were used for each acid digestion reaction. The resulting CO_2 analyte, sufficient for two replicate analyses, was then dried using a − 80 °C ethanol trap.

The triple oxygen Isotope composition of CO_2 from the carbonate digestions, as well as the CO_2 gas used for the experiments, were measured at the University of Göttingen using an Aerodyne TILDAS laser spectrometer connected to a custom-built dual inlet system. The instrumentation and measurement procedure are detailed in Bajnai et al. (2023). The measured $\delta^{18}O$ and $\Delta'^{17}O$ values of the CO_2 were scaled relative to the NBS-18 ($\delta^{18}O_{CO2} = 17.324‰$, $\Delta'^{17}O_{CO2} = -100$ ppm) and IAEA-603 ($\delta^{18}O_{CO2} = 39.012‰$, $\Delta'^{17}O_{CO2} = -147$ ppm) values reported by Wostbrock et al. (2020b). In practice, we first determined the triple oxygen isotope composition of our two in-house reference gases, light CO_2 and heavy CO_2, relative to NBS-18 and IAEA-603. Then, we used these in-house reference gases to scale the sample measurements. The reason for this two-step correction is that we can measure more reference gas replicates (such measurements are fully automated) than carbonate reference materials, and thus using the reference CO_2 gases makes the long-term comparison of data more reliable.

To validate our scaling method and ensure the stability of our acid digestion procedure over time, we included measurements of a Devils Hole subaqueous cave carbonate as an internal carbonate standard. Our sample, DH-11 19.7, is not exactly the same as DHC2–8 investigated by Wostbrock et al. (2020a), but their dual clumped isotope compositions are identical, suggesting that both samples grew under similar conditions (Bajnai et al., 2021). Although the $\delta^{18}O$ value of DH-11 19.7 is approximately 0.5‰ lower than that of DHC2–8, we expect their $\Delta'^{17}O$ values to be similar because we use the slope of the meteoric water line for λ_{RL} (Eq. (7)),

To determine the oxygen isotope composition of the carbonate, we needed the acid fractionation factors (AFF) for $^{17}O/^{16}O$ and $^{18}O/^{16}O$ for $BaCO_3$ at 25 °C. Unfortunately, there is no ^{17}O AFF data available for witherite. Therefore, we used the calcite AFFs instead as an approximation. Specifically, we used the AFF of Kim et al. (2007) for $^{18}O/^{16}O$ ($\alpha^{18}_{CO2(acid)/calcite} = 1.01025$ at 25 °C) and the AFF of Wostbrock et al. (2020b) for $^{17}O/^{16}O$ ($\theta_{CO2(acid)/calcite} = 0.523$). The measured CO_2 isotope compositions are listed in the supplementary material, allowing for recalculating the isotope values once the witherite acid fractionation factors are determined.

In addition to the laser spectroscopic analyses, we measured the carbonate precipitates using isotope ratio mass spectrometry (IRMS) to determine their $\delta^{13}C$ values. The IRMS measurements were performed at the University of Göttingen. Carbonates were digested in phosphoric acid at 72 °C using a ThermoFischer KIEL IV carbonate preparation device, and the resulting CO_2 was measured using a Finnigan Delta Plus isotope ratio mass spectrometer. The data were corrected using two calcite standards, NBS-18 and IAEA-603, which were measured alongside the samples.

2.3. Isotope analyses of waters

The triple oxygen isotope compositions of the purified tap water and the barium-hydroxide-bound water were measured on O_2 gas derived from H_2O fluorination (Baker et al., 2002; Barkan and Luz, 2005). To

extract mineral-bound water from crystalline $Ba(OH)_2 \times 8H_2O$, we used a routine similar to extracting water from gypsum (Herwartz et al., 2017). First, a few grams of the salt were placed in a glass vial, which was then briefly evacuated for a few seconds. Then, the salt was heated to 400 °C in a vacuum, converting it to BaO. The liberated mineral-bound water was quantitatively collected in a liquid-nitrogen-chilled 6-mm-outer-diameter glass vial.

The Isotope measurements were performed at the University of Cologne on a ThermoFisher MAT 253 gas source isotope ratio mass spectrometer. The O_2 triple oxygen isotope data were corrected using in-house water standards calibrated against VSMOW-2/SLAP-2 (Herwartz et al., 2017; Schoenemann et al., 2013). During each analytical session, at least two laboratory standards were analyzed alongside the samples, namely, Pitztal ($\delta^{18}O = -13.86‰$; $\Delta'^{17}O = 26$ ppm), BW ($\delta^{18}O = 18.13‰$; $\Delta'^{17}O = -86$ ppm), and NEEM ($\delta^{18}O = -26.04$; $\Delta'^{17}O = 36$ ppm).

2.4. Quantum-chemical calculations

The equilibrium triple oxygen isotope exponent θ^{eq}_{H2O/OH^-} can be determined by:

$$\theta^{eq}_{H_2O/OH^-} = \kappa_{H_2O} + (\kappa_{H_2O} - \kappa_{OH^-}) \cdot \frac{ln\left({}^{18}\beta_{OH^-}\right)}{ln\left({}^{18}\alpha_{H_2O/OH^-}\right)} \quad (10)$$

$$\kappa = \frac{ln\left({}^{17}\beta\right)}{ln\left({}^{18}\beta\right)} \quad (11)$$

The theoretical parameter β relates to the hypothetical isotope equilibrium between either H_2O or aqueous OH^- and an ideal gaseous mono-atomic oxygen with no thermodynamic affinity for one oxygen isotope over another (Cao and Liu, 2011; Guo and Zhou, 2019; Hayles et al., 2018; Richet et al., 1977; Schauble, 2004). For the calculations using Eq. (10), the value of κ_{H2O} was estimated to be 0.5299 at 25 °C (Cao and Liu, 2011), ${}^{18}\beta_{OH^-}$ and ${}^{18}\alpha_{H2O/OH^-}$ were estimated to be 1.0519 and 1.0235 at 25 °C (Zeebe, 2020), respectively. We calculated the only remaining unknown parameter, κ_{OH^-} (Eq. (11)). Specifically, we simulated the aqueous OH^- by water cluster $OH^-\bullet(H_2O)_{32}$, and determined the reduced partition function ratio (f_r) of $OH^-\bullet(H_2O)_{32}$ (Bigeleisen and Goeppert Mayer, 1947; Urey, 1947), giving the values of ${}^{17}\beta_{OH^-}$ and ${}^{18}\beta_{OH^-}$ (Cao and Liu, 2011):

$$f_r = \prod_i^l \frac{u_i^*}{u_i} \cdot \frac{e^{-u_i^*/2}}{e^{-u_i/2}} \cdot \frac{1 - e^{-u_i}}{1 - e^{-u_i^*}} \quad (12)$$

where l is the number of vibrational degrees of freedom and equals to *3N-6* in this case, N is the number of atoms in water cluster $OH^-\bullet(H_2O)_{32}$, and u_i is equal to $hc\omega_i/k_BT$, where h is the Planck-constant, c is the speed of light, ω_i is the i^{th} normal vibration mode, k_B is the Boltzmann-constant and T is temperature. The terms marked with an asterisk refer to the isotopologues containing the heavy isotopes. The vibrational frequencies in Eq. (12) were calculated by B3LYP method with 6–311+G(2df,p) basis set according to our previous work (Cao and Liu, 2011).

In addition to the equilibrium parameters, we also calculated the kinetic isotope effect (KIE) superimposed on the OH^- reacting with CO_2. According to transition state theory, the kinetic isotope effect can be calculated by:

$$KIE = \frac{K_H^\ddagger}{K_L^\ddagger} = \frac{s_L^\ddagger}{s_H^\ddagger} \frac{s_H^R}{s_L^R} \frac{f_r^\ddagger}{f_r^R} \frac{\nu_H^\ddagger}{\nu_L^\ddagger} \quad (13)$$

in which s is symmetry number, f_r is the reduced partition function ratio, and ν is the imaginary frequency, subscripts L and H refer to light and heavy isotopes, respectively, and ‡ and R denote the transition state and reactant, respectively (Bigeleisen and Wolfsberg, 1957). In our case, all symmetry numbers equal to one, and f_r can be calculated using Eq. (13). The reactant was simulated by water cluster $CO_2\bullet OH^-\bullet(H_2O)_{32}$. Berny algorithm was employed to search the transition state. It is more difficult to locate a transition state than to locate an equilibrium structure (Zeebe, 2020). Imaginary frequency and IRC (intrinsic reaction coordinate) analysis were carried out to guarantee that the located structure is the wanted transition state. Once the transition state is obtained, $f_r^\ddagger$ and $\nu^\ddagger$ can be determined. Combining with the f_r value for $OH^-\bullet(H_2O)_{32}$, ${}^{18}KIE_{OH^-}$ and $\theta^{KIE}_{OH^-}$ can be estimated. The Gaussian09 software package is used for all quantum-chemical calculations in this study (Frisch et al., 2009). All computations were executed at a temperature of 25 °C.

3. Results

The CO_2 triple oxygen isotope measurements were performed in two measurement periods. The triple oxygen isotope composition of light CO_2 and heavy CO_2 was determined in the "2023-09-18 to 2023-10-08" measurement period, based on ten replicate analyses (from five acid digestion reactions) of NBS-18 and IAEA-603 (Fig. S1), and 24 and 26 replicate analyses of light CO_2 and heavy CO_2, respectively (Fig. S2b). During this measurement period, the repeatability of the $\delta^{18}O$ and $\Delta'^{17}O$ analyses was ±0.023‰ and ± 8 ppm for the CO_2 reference gases and ± 0.094‰ and ± 8 ppm for the carbonate standards. The scaled oxygen isotope composition of light CO_2 was determined to be $\delta^{18}O = -1.509$ (±0.022)‰ and $\Delta'^{17}O = -141(\pm 8)$ ppm, while heavy CO_2 was $\delta^{18}O = 76.820(\pm 0.023)‰$ and $\Delta'^{17}O = -213(\pm 8)$ ppm. Using the light and heavy CO_2 to scale DH-11 19.7 within the same measurement period yielded a carbonate $\delta^{18}O$ value of 13.979(±0.063)‰ and a $\Delta'^{17}O$ value of −54(±9) ppm ($N = 6$). For DHC2–8, Wostbrock et al. (2020a) got $\delta^{18}O = 14.621‰$ and $\Delta'^{17}O = -43(\pm 7)$ ppm.

The carbonate samples were measured in two measurement periods: "2023-07-01 to 2023-08-01" and "2023-09-18 to 2023-10-18" (see above). For the earlier measurement period, the repeatability of the light and heavy CO_2 $\delta^{18}O$ and $\Delta'^{17}O$ analyses was ±0.023‰ and ± 9 ppm, respectively (Fig. S2a). Each CO_2 aliquot from the carbonate acid digestion reactions was measured up to twice. Because the two replicates from a single CO_2 aliquot did not show a larger difference in their $\delta^{18}O$ and $\Delta'^{17}O$ values than the repeatability of subsequent analyses of the same carbonate sample (Fig. S3a), we combined all replicate

Table 1
Results of the witherite carbon and triple oxygen isotope measurements.

Sample	$\delta^{13}C$ (‰, VPDB)*	$\delta^{18}O$ (‰, VSMOW)*	$\delta^{18}O$ (‰, VSMOW)‡	$\Delta'^{17}O$ (ppm)‡
Exp. A	−4.574 (±0.025)	6.191(±0.005)	5.826(±0.107)	−173(±4)
Exp. B	−5.197 (±0.042)	6.084(±0.064)	5.935(±0.041)	−182(±8)
Exp. C	−5.035 (±0.050)	6.187(±0.040)	–	–
Exp. D	−5.252 (±0.018)	5.885(±0.032)	–	–
Exp. E	−5.291 (±0.150)	6.035(±0.082)	5.916(±0.089)	−179(±6)
Exp. F	−5.419 (±0.091)	6.078(±0.111)	–	–
Exp. G	−5.147 (±0.011)	6.062(±0.032)	5.820(±0.061)	−185(±8)
Exp. H	−5.250 (±0.004)	6.040(±0.057)	5.899(±0.052)	−181(±5)
Exp. I	−5.374 (±0.028)	5.948(±0.027)	5.886(±0.045)	−172(±10)
Exp. J	−5.976 (±0.089)	7.938(±0.008)	–	–
Exp. K	−5.242 (±0.004)	6.084(±0.012)	–	–

The oxygen isotope values are corrected for acid fractionation (see text for details). Errors represent ±1 S.D. The results are deposited in Tables S2–S4. *Data from IRMS analyses, ‡Data from laser spectroscopy.

analyses of the same sample (Tables 1–2). The triple oxygen isotope measurements of the tank CO_2 used for the precipitation experiments ($N = 8$) yielded a $\delta^{18}O$ value of 32.132(±0.031)‰ and a $\Delta'^{17}O$ value of −116(±6) ppm.

The reproducibility of the IRMS measurements was ±0.03‰ for $\delta^{13}C$ and ± 0.05‰ for $\delta^{18}O$. The difference between the mass-spectrometric and laser spectroscopic $\delta^{18}O$ analyses was <0.4‰ (Table 1). For the isotope fractionation calculations, we only consider the laser spectroscopy data.

Triple oxygen isotope measurements of the purified tap water that was used for the experiments yielded a $\delta^{18}O$ value of −7.92(±0.3)‰ and a $\Delta'^{17}O$ value of 25(±8) ppm. The barium-hydroxide salt had $\delta^{18}O = -6.93(\pm0.3)$‰ and $\Delta'^{17}O = 33(\pm9)$ ppm. The errors reported here correspond to the long term reproducibility of the method used (Herwartz et al., 2017). Because the $Ba(OH)_2$ x $8H_2O$ salt contributes approximately 4% of the total oxygen pool of the saturated solution, its impact on the solution's oxygen isotope composition needs to be considered (c.f., Bajnai and Herwartz, 2021). In our case, the $\Delta'^{17}O$ of the salt-bound water is indistinguishable within errors from the tap water. According to a mass balance, the addition of barium-hydroxide salt to the water changed the solution's $\delta^{18}O$ by <0.1‰, which is within the measurement error. Therefore, we consider the isotope composition of the tap water to be representative of the solution's composition.

The quantum chemical computations yielded a κ_{OH^-} of 0.53004. By inserting this value into Eq. (10), we determined the equilibrium triple oxygen exponent ($\theta^{eq.}_{H2O/OH^-}$) to be 0.5296 at 25 °C. For the kinetic isotope effect superimposed on the reacting hydroxide ion, our calculations yielded −13.5‰ (= $^{18}KIE_{OH^-}$) and 0.5124 (= $\theta^{KIE}_{OH^-}$). The computed vibrational frequencies are shown in Tables S5–S6.

4. Discussion

4.1. How much of the dissolved CO_2 had been consumed in the experiments?

After quantitative precipitation of CO_2, one can expect that the $\delta^{13}C$ of the carbonate is identical to that of the CO_2, given that CO_2 is the only carbon-bearing dissolved species. However, our $BaCO_3$ precipitates show some deviation in $\delta^{13}C$ compared to the CO_2. Most $BaCO_3$ precipitates have 0.1–0.4‰ lower $\delta^{13}C$ than the CO_2 and uniform $\delta^{18}O$ values. A similar $\delta^{13}C$ fractionation was observed by Bajnai and Herwartz (2021). Experiments A and J show up to 0.8‰ higher $\delta^{13}C$ values than the CO_2, accompanied by, relative to the rest of the experiments, elevated $\delta^{18}O$ by up to 8‰ (Fig. 2a).

Air CO_2 has a $\delta^{13}C$ value of approximately −8‰, which is roughly 4‰ lower than the CO_2 gas used in our experiments. The inclusion of air CO_2 precipitates in our experiments would shift the $\delta^{13}C$ values of the bulk carbonate towards more negative values. To account for the observed 0.1–0.4‰ $\delta^{13}C$ offsets, we would need an approximate contribution of 20–30% from such carbonates. Isotopically light CO_2 from breathing may have even lowered the $\delta^{13}C$ of the ambient lab air CO_2, requiring a smaller contribution from air CO_2 precipitates to shift the $\delta^{13}C$ values of the bulk carbonates. It is possible that the purified water used to rinse the precipitates in step 7 contained some dissolved inorganic carbon (DIC), which could have reacted with any remaining solution. Additionally, it is conceivable that air CO_2 reacted with barium hydroxide after the precipitates were dried and removed from the glove box. In the latter two scenarios, the maximum amount of contaminating carbonate would be what could precipitate from the remaining solution or barium hydroxide salt on the filter paper. Even imagining an unlikely scenario that the filter paper is soaked with a fully saturated solution, approximately 0.05 cm^3 of solution could have remained in it, holding ca. 10^{-5} mol barium-hydroxide. This amount of barium hydroxide could yield a maximum of 2 mg of $BaCO_3$, contributing to a max 10% contamination. We emphasize that this max 10% estimate is an unrealistic worst-case scenario, and even this overestimation cannot explain the small negative shift in $\delta^{13}C$. Finally, there is no correlation between the apparent % yields of the experiments (Table S1) and the measured isotope compositions, further underlining that the precipitates are not contaminated.

A more likely explanation for the negative $\delta^{13}C$ offsets is the preferential reaction of light CO_2 during hydroxylation (c.f., Sade and Halevy, 2017). Specifically, Christensen et al. (2021) model an extreme isotopic distillation effect during the precipitation of carbonate induced by the absorption of atmospheric CO_2 in natural high-pH ponds. They argue that the progressive hydroxylation of light CO_2 can lead to residual CO_2 that is isotopically heavy, i.e., yielding $\delta^{13}C_{CO2}$ values up to 100‰ (!) (see Fig. 12 g in Christensen et al. (2021)). Therefore, any but a 100% precipitation would lead to lower-than-expected carbonate $\delta^{13}C$ values in our witherite samples. The corresponding effect for $\delta^{18}O_{CO2}$ is modeled to be negligible (see Fig. 12d in Christensen et al. (2021)) consistent with a small hydroxylation $^{18}KIE_{CO2}$ calculated from literature data herein (see Chapter 4.3).

On the other hand, losing light CO_2 during the preparation of the break seal tubes would lead to CO_2 in the tubes enriched in heavy isotopes (^{13}C and ^{18}O). Subsequently, carbonates that precipitate from such fractionated CO_2 (even if the precipitation in the following experimental step is quantitative) would yield higher-than-expected carbonate $\delta^{13}C$ and $\delta^{18}O$ values. Regardless of the observed positive and negative $\delta^{13}C$ offsets, there is no correlation between the $\delta^{13}C$ and the $\Delta'^{17}O$ values of the precipitates. This suggests that any superimposed kinetic effect resulting from non-quantitative precipitation is not resolvable in the triple oxygen isotope values. For calculating the isotope fractionation factors, we use the average composition of the samples (Exp. A, B, E, G, H, and I; Table 1).

Table 2
Overview of the triple oxygen isotope values used to calculate the composition of the reacting hydroxide-ion ($OH^- + KIE_{OH^-}$) in the experiments.

Species	$\delta^{18}O$ (‰ VSMOW)	$\Delta'^{17}O$ (ppm)
$BaCO_3$	5.88(±0.05)	−179(±5)
H_2O	−7.92(±0.71)	25(±5)
CO_2	32.13(±0.03)	−116(±6)
$OH^- + KIE_{OH^-}$	−46.63(±0.16)	220(±20)

The effective composition of the OH^- is calculated using Eq. (8), assuming that the KIE_{CO2} is 0, corresponding to quantitative CO_2 consumption during the reaction. To account for uncertainties in the triple oxygen isotope values of both the precipitates and the CO_2, we employed a Monte Carlo approach to propagate these into the uncertainty of the calculated composition of the hydroxide ion.

4.2. Triple oxygen isotope fractionation in the H_2O–OH^- system

Using the mass balance in Eq. (8), the measured water and measured $BaCO_3$ compositions, we calculated the triple oxygen isotope composition of the hydroxide ion participating in the hydroxylation reaction ($OH^- + KIE_{OH^-}$), resulting in a $\delta^{18}O$ of −46.59(±0.21)‰ and a $\Delta'^{17}O$ of 220(±21) ppm (Figs. 3–4, Table 2). Experimental studies can only determine the effective isotope fractionation between water and the OH^- with kinetics (KIE_{OH^-}) superimposed on the equilibrium fractionation. We observe a fractionation factor between H_2O and OH^- at 22 °C of 39.8(±0.2)‰, which agrees with previous experimental estimates (Bajnai and Herwartz, 2021). Our experimental estimates on the effective $^{18}O/^{16}O$ oxygen isotope fractionation between H_2O and the reacting $OH^-$are approximately 15‰ to 20‰ higher than the equilibrium modeled by Zeebe (2020) (Fig. 3).

Knowledge of the triple oxygen isotope composition of water and coexisting OH^- allows calculating the triple oxygen isotope fractionation exponent θ_{H2O/OH^-}. The calculated effective triple oxygen isotope exponent $\theta^{effective}_{H2O/OH^-}$ of 0.523(±0.001) can be understood as the combination of an $\theta^{eq.}$ and θ^{KIE} (Fig. 4). For $\theta^{eq.}_{H2O/OH^-}$ Guo and Zhou (2019) estimated 0.5296, based on statistical thermodynamics calculations. Our

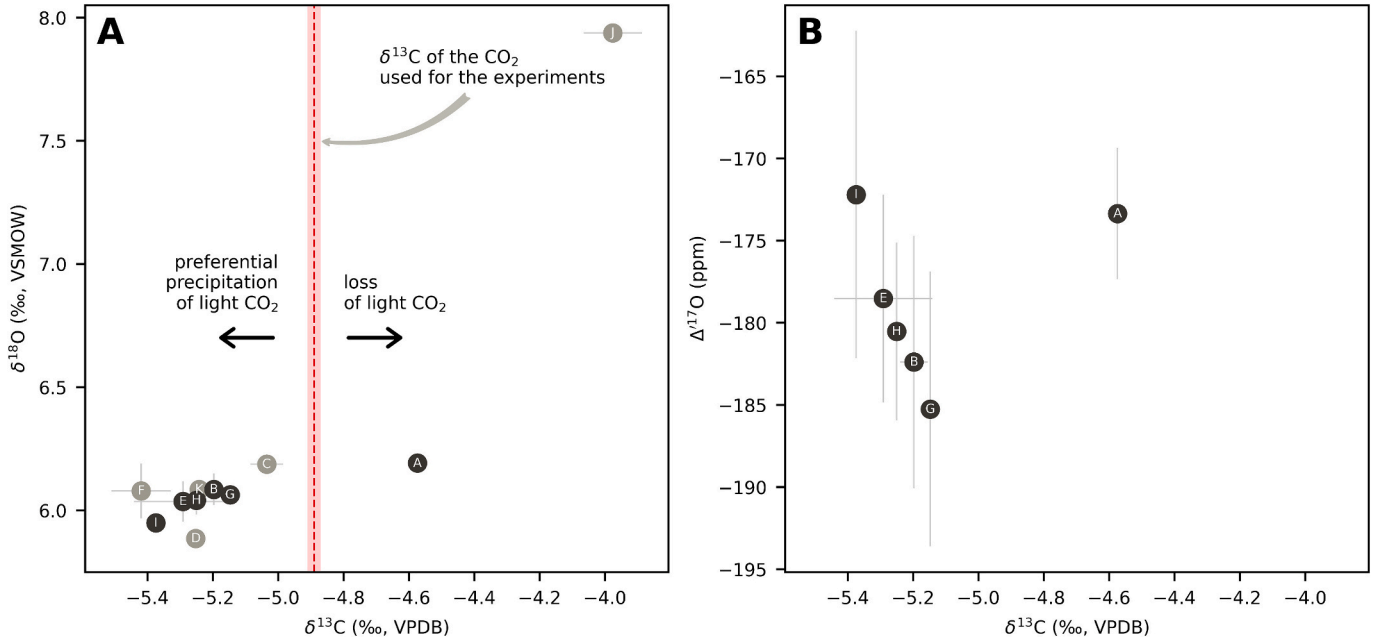

Fig. 2. The oxygen and carbon isotope composition of the $BaCO_3$ precipitates. (A) Crossplot between $\delta^{18}O$ and $\delta^{13}C$ values. Black circles are the experiments that were measured for triple oxygen isotopes. (B) Crossplot between $\Delta'^{17}O$ and $\delta^{13}C$ values.

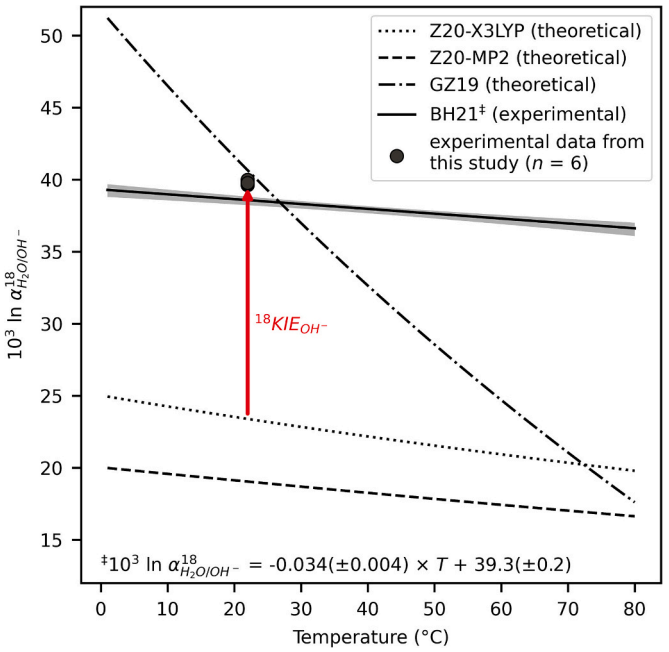

Fig. 3. Oxygen $^{18}O/^{16}O$ isotope fractionation between water and aqueous OH^-. The experimental data from this study are consistent with the previous experimental estimates of Bajnai and Herwartz (2021). The Bajnai and Herwartz (2021) equation shown here (solid line) is recalculated without a correction for the difference in acid fractionation factors between calcite and witherite, i.e., the carbonate $\delta^{18}O$ values are 1.03‰ higher than initially published. Theoretical equilibrium curves (dashed, dotted) are from Zeebe (2020) and (dash-dotted) from Guo and Zhou (2019).

revised theoretical calculations confirm this value. As can be expected for rapid ion exchange reactions, the theoretical results are close to the experimental $\theta_{liquid/vapor}$ of 0.529 (Barkan and Luz, 2005). Consequently, the $\Delta'^{17}O$ value of the OH^- in equilibrium with water is lower compared to the parent water (Fig. 4).

Bajnai and Herwartz (2021) argued that the KIE is related to the preferential reaction of the light $^{16}OH^-$ during CO_2 hydroxylation. The triple oxygen isotope slope for the kinetic isotope effect superimposed on the reacting OH^- — considering that it behaves like a diffusing molecule — can be estimated from Graham's law (Graham, 1864):

$$\theta_{OH^-}^{Graham} = \frac{ln\left(\frac{M_{16_{OH^-}}}{M_{17_{OH^-}}}\right)}{ln\left(\frac{M_{16_{OH^-}}}{M_{18_{OH^-}}}\right)} = 0.514 \quad (14)$$

The respective $\theta_{OH\text{-}}^{Graham}$ value of 0.514 is identical to the $\theta_{OH\text{-}}^{KIE}$ value we estimated by combining the equilibrium and the measured effective OH^- fractionation factors (Fig. 4). This low $\theta_{OH\text{-}}^{KIE}$ drives the $\Delta'^{17}O_{OH\text{-}}$ of the effectively reacting OH^- to ca. 230 ppm higher values. Guo and Zhou (2019) modeled the $\theta_{OH\text{-}}^{KIE}$ to be 0.4951 (their Table 3; line 4), increasing the $\Delta'^{17}O_{OH\text{-}}$ to even higher values. We also re-examined the $\theta_{OH\text{-}}^{KIE}$ using transition state theory and found a theoretical value of 0.5124, which is very close to our empirical constraints. The transition state theory also provides the magnitude of the $^{18}KIE_{OH\text{-}} = -13.5‰$, roughly consistent with the −16.4‰ derived from combining our empirical results with calculated equilibrium $\alpha_{H2O/OH\text{-}}^{18}$ using the X3LYP model of Zeebe (2020) (Fig. 4).

4.3. Implications for CO_2 hydroxylation kinetics

Paleotemperature reconstructions using classic $\delta^{18}O$–T calibrations require precipitation close to equilibrium. Samples such as our witherite precipitates are far removed from the equilibrium point (Fig. 4). They comprise much lower $\delta^{18}O$ and $\Delta'^{17}O$ than expected from equilibrium, making them inappropriate for temperature reconstructions. A correction scheme, similar to what was proposed for clumped isotopes by Bajnai et al. (2020), would allow 'seeing through' kinetic processes and reconstructing accurate growth temperatures using disequilibrium carbonate samples. Such a correction requires accurate knowledge of the characteristic fractionation slope for the respective kinetic process (Herwartz, 2021). With this goal in mind, the proposed hydroxylation slopes in triple oxygen isotope space are reassessed.

Guo and Zhou (2019) model a slope of 0.548(±0.001) for pure hydroxylation, with the error reflecting a small temperature effect (5–35 °C). Using a much simpler approach, Herwartz (2021) suggested a

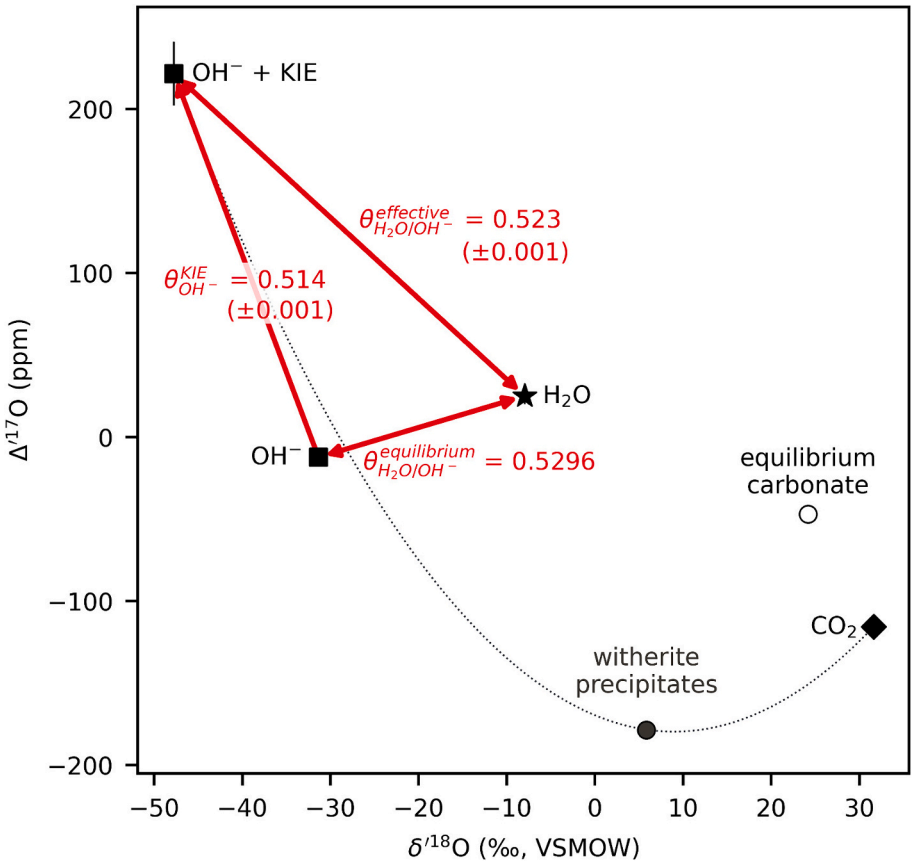

Fig. 4. Triple oxygen isotope fractionation between H_2O and OH^-. The dotted black line depicts the mass balance from Eq. (8). The values used for the mass balance calculations are listed in Table 2. The position of the equilibrium carbonate is calculated using Wostbrock et al. (2020a). The $\delta^{18}O$ value of the equilibrium OH^- is based on the X3LYP model of Zeebe (2020).

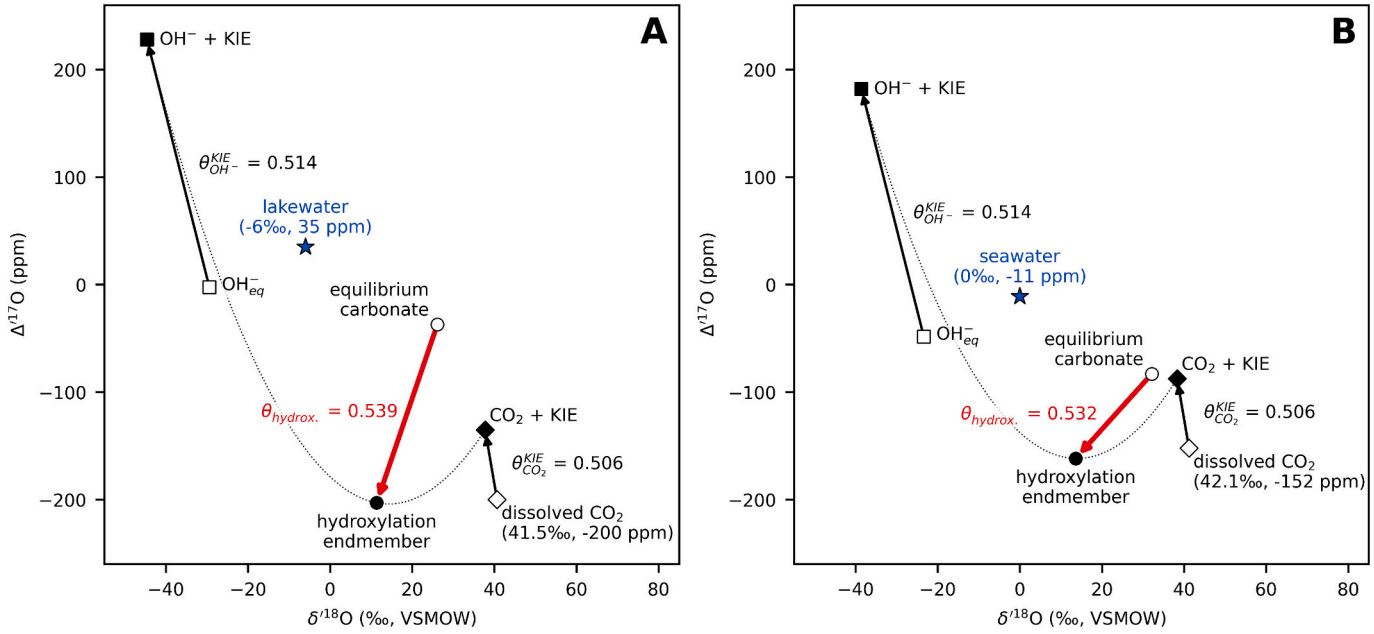

Fig. 5. The slope of CO_2 hydroxylation depends on the composition of the water and the CO_2. (A) Model for an alkaline lake, where air CO_2 is absorbed via hydroxylation. (B) Model for a marine environment where dissolved CO_2 is converted to bicarbonate via hydroxylation. The equilibrium isotope composition of the dissolved OH^- is calculated following Zeebe (2020) and this study, whereas that of dissolved CO_2 is calculated according to Guo and Zhou (2019). We discuss the extent of the kinetic isotope effects on dissolved OH^- and CO_2 in the main text. The isotope composition of a carbonate forming at 22 °C is calculated using the calcite equation in Hayles et al. (2018). Finally, the position of the hydroxylation end member is calculated using a mass balance between the reacting OH- and CO_2 (Eq. (8)).

$\theta_{hydroxylation}$ of 0.535 (at 25 °C) but noted the uncertainty with respect to the KIE superimposed on the OH^- and the CO_2.

In our experiments, the KIE_{OH^-} is fully expressed, but the KIE_{CO2} is close to 0, which is not the case in most natural settings. Christensen et al. (2023, 2021) compiled in their Table 7 a list of high-pH (pH > 10) precipitations, where besides the isotope composition of the mineral, the composition of the precipitating CO_2 and the water are also known. In these precipitates, both the KIE_{OH^-} and KIE_{CO2} are expressed. By rearranging Eq. (8) and calculating the $\delta^{18}O_{OH^-}^{effective}$ from the isotope composition of the ambient water, we can estimate an average KIE_{CO2} of −3(±2)‰. A corresponding θ_{CO2}^{KIE} can be estimated from Graham's law to be 0.506.

It should be stressed that a uniform $\theta_{hydroxylation}$ does not exist. That is, the isotope composition of CO_2 and ambient water affects the hydroxylation slope, and thus, some variation is expected for individual settings. Fig. 5 demonstrates this using two examples, in which carbonates precipitate via pure hydroxylation. In these examples, the KIE for both CO_2 and OH^- are fully expressed. In alkaline lakewater, where atmospheric CO_2 is absorbed from air, the $\theta_{hydroxylation}$ is 0.539. In seawater, where CO_2 is assumed to be in full equilibrium with the water the $\theta_{hydroxylation}$ is estimated as 0.532. Both estimates are slightly temperature-dependent because the equilibrium fractionation is temperature-dependent. However, because $OH^-_{eq.}$ and dissolved CO_2 evolve in opposite directions, the net temperature effect on $\theta_{hydroxylation}$ is small.

5. Conclusions

In this study, we modeled the equilibrium triple oxygen isotope fractionation between H_2O and the dissolved hydroxide ion (OH^-) and quantified the kinetic isotope effects during hydroxylation (CO_2 and OH^-). Specifically, we performed ab initio quantum chemical modeling to determine the equilibrium fractionation between H_2O and ambient OH^-. To estimate the kinetic isotope effect for a purely kinetic process, we performed witherite precipitation experiments in which CO_2 gas was reacted with a high-pH barium-hydroxide solution, forming $BaCO_3$. Our experimental setup ensured rapid and quantitative precipitation of CO_2 entirely via hydroxylation. From the measured triple oxygen isotope composition of the precipitates, the CO_2, and the solution, we calculated the effective oxygen isotope fractionation factors between water and OH^- using a simple mass balance.

Our quantum chemical modeling confirms the previously suggested equilibrium $\theta_{H2O/OH^-}^{eq.}$ of 0.5296 at 25 °C. Using the estimated equilibrium and the measured isotope values, we calculated kinetic isotope fractionation factors (KFF) for OH^-. Our data on the $^{18}O/^{16}O$ fractionation validate previous experimental estimates and show a kinetic isotope effect superimposed on the reacting OH^- of −16.4‰ (= $^{18}KFF_{OH^-}$). Similarly, the reacting OH^- has a $\Delta'^{17}O$ value ca. 230 ppm higher than what is expected for equilibrium. In triple oxygen isotope space, the slope between the equilibrium and kinetic OH^- is 0.514 (= θ_{H2O/OH^-}^{KIE}). Combining the equilibrium and kinetic estimates with literature data on high pH precipitates where the isotope composition of the reactants was known, we estimated the kinetic isotope effect superimposed on the reacting CO_2 to be approximately −3‰ (= $^{18}KFF_{CO2}$).

Finally, our results enable a more accurate modeling of kinetic isotope effects in triple oxygen isotope space, particularly for the slope of hydroxylation. The $\theta_{hydroxylation}$ is dependent on the isotope composition of the ambient water, CO_2, and the temperature. For carbonates growing in seawater, we estimate it to be 0.532 at 25 °C.

CRediT authorship contribution statement

David Bajnai: Writing – original draft, Visualization, Validation, Methodology, Investigation, Formal analysis, Data curation, Conceptualization. **Xiaobin Cao:** Writing – review & editing, Methodology, Investigation, Formal analysis. **Swea Klipsch:** Formal analysis. **Andreas Pack:** Writing – review & editing, Validation, Resources, Data curation. **Daniel Herwartz:** Writing – original draft, Methodology, Investigation, Funding acquisition, Formal analysis.

Declaration of competing interest

The authors declare that they have no known competing financial interests or personal relationships that could have appeared to influence the work reported in this paper.

Data availability

The supplementary data and the computer codes used to create the figures in the manuscript are deposited at GitHub (https://github.com/davidbajnai/hydroxylation) and Zenodo (https://doi.org/10.5281/zenodo.10830205).

Acknowledgments

We thank Dennis Kohl and Tommaso Di Rocco (University of Göttingen), and Jochen Scheld (University of Cologne) for their technical support in the laboratory. We also thank Lothar Laake and the GZG Zentralwerkstatt for their help with the experimental setup. Comments from two anonymous reviewers helped improve this manuscript. This research was funded by the DFG via grants HE 6357/2-2 and HE 6357/4-1.

Appendix A. Supplementary material

The Supplementary Material contains Fig. S1, showing the $\delta^{18}O$ and $\Delta'^{17}O$ values of NBS-18 and IAEA-603; Fig. S2, showing the unscaled CO_2 triple oxygen isotope measurements; and Fig. S3, showing the $\Delta'^{17}O$ and $\delta^{18}O$ values of the precipitation experiments. Table S1 shows the parameters and yields of the precipitation experiments. Data for the carbonate oxygen isotope measurements from laser spectroscopy (Tables S2–S3) and mass spectrometry (Table S4) are available as separate files. Tables S5 and S6 contain the calculated vibrational frequencies. Supplementary data to this article can be found online at https://doi.org/10.1016/j.chemgeo.2024.122059.

References

Bajnai, D., Herwartz, D., 2021. Kinetic oxygen isotope fractionation between water and aqueous OH^- during hydroxylation of CO_2. ACS Earth Space Chem. 5, 3375–3384. https://doi.org/10.1021/acsearthspacechem.1c00194.

Bajnai, D., Fiebig, J., Tomašových, A., Milner Garcia, S., Rollion-Bard, C., Raddatz, J., Löffler, N., Primo-Ramos, C., Brand, U., 2018. Assessing kinetic fractionation in brachiopod calcite using clumped isotopes. Sci. Rep. 8, 533. https://doi.org/10.1038/s41598-017-17353-7.

Bajnai, D., Guo, W., Spötl, C., Coplen, T.B., Methner, K., Löffler, N., Krsnik, E., Gischler, E., Hansen, M., Henkel, D., Price, G.D., Raddatz, J., Scholz, D., Fiebig, J., 2020. Dual clumped isotope thermometry resolves kinetic biases in carbonate formation temperatures. Nat. Commun. 11, 4005. https://doi.org/10.1038/s41467-020-17501-0.

Bajnai, D., Coplen, T.B., Methner, K., Löffler, N., Krsnik, E., Fiebig, J., 2021. Devils Hole calcite was precipitated at ±1 °C stable aquifer temperatures during the last half million years. Geophys. Res. Lett. 48 https://doi.org/10.1029/2021gl093257 e2021GL093257.

Bajnai, D., Pack, A., Arduin Rode, F., Seefeld, M., Surma, J., Di Rocco, T., 2023. A dual inlet system for laser spectroscopy of triple oxygen isotopes in carbonate-derived and air CO_2. Geochem. Geophys. Geosyst. 24 https://doi.org/10.1029/2023GC010976 e2023GC010976.

Baker, L., Franchi, I.A., Maynard, J., Wright, I.P., Pillinger, C.T., 2002. A technique for the determination of $^{18}O/^{16}O$ and $^{17}O/^{16}O$ isotopic ratios in water from small liquid and solid samples. Anal. Chem. 74, 1665–1673. https://doi.org/10.1021/ac010509s.

Barkan, E., Luz, B., 2005. High precision measurements of $^{17}O/^{16}O$ and $^{18}O/^{16}O$ ratios in H_2O. Rapid Commun. Mass Spectrom. 19, 3737–3742. https://doi.org/10.1002/rcm.2250.

Bigeleisen, J., Goeppert Mayer, M., 1947. Calculation of equilibrium constants for isotopic exchange reactions. J. Chem. Phys. 15, 261–267. https://doi.org/10.1063/1.1746492.

Bigeleisen, J., Wolfsberg, M., Prigogine, I., 1957. Theoretical and experimental aspects of isotope effects in chemical kinetics. In: Debye, P. (Ed.), Advances in Chemical Physics. Wiley, pp. 15–76. https://doi.org/10.1002/9780470143476.ch2.

Cao, X., Liu, Y., 2011. Equilibrium mass-dependent fractionation relationships for triple oxygen isotopes. Geochim. Cosmochim. Acta 75, 7435–7445. https://doi.org/10.1016/j.gca.2011.09.048.

Christensen, J.N., Watkins, J.M., Devriendt, L.S., DePaolo, D.J., Conrad, M.E., Voltolini, M., Yang, W., Dong, W., 2021. Isotopic fractionation accompanying CO_2 hydroxylation and carbonate precipitation from high pH waters at the Cedars, California, USA. Geochim. Cosmochim. Acta 301, 91–115. https://doi.org/10.1016/j.gca.2021.01.003.

Christensen, J.N., Watkins, J.M., Devriendt, L.S., DePaolo, D.J., Conrad, M.E., Voltolini, M., Yang, W., Dong, W., 2023. Corrigendum to "Isotopic fractionation accompanying CO_2 hydroxylation and carbonate precipitation from high pH waters at the Cedars, California, USA" [Geochim. Cosmochim. Acta 301 (2021) 91–115]. Geochim. Cosmochim. Acta 343, 416–419. https://doi.org/10.1016/j.gca.2022.09.022.

Daëron, M., Drysdale, R.N., Peral, M., Huyghe, D., Blamart, D., Coplen, T.B., Lartaud, F., Zanchetta, G., 2019. Most Earth-surface calcites precipitate out of isotopic equilibrium. Nat. Commun. 10, 429. https://doi.org/10.1038/s41467-019-08336-5.

Davies, A.J., Guo, W., Bernecker, M., Tagliavento, M., Raddatz, J., Gischler, E., Flögel, S., Fiebig, J., 2022. Dual clumped isotope thermometry of coral carbonate. Geochim. Cosmochim. Acta 338, 66–78. https://doi.org/10.1016/j.gca.2022.10.015.

Davies, A.J., Brand, U., Tagliavento, M., Bitner, M.A., Bajnai, D., Staudigel, P., Bernecker, M., Fiebig, J., 2023. Isotopic disequilibrium in brachiopods disentangled with dual clumped isotope thermometry. Geochim. Cosmochim. Acta 359, 135–147. https://doi.org/10.1016/j.gca.2023.08.005.

Devriendt, L.S., Watkins, J.M., McGregor, H.V., 2017. Oxygen isotope fractionation in the $CaCO_3$–DIC–H_2O system. Geochim. Cosmochim. Acta 214, 115–142. https://doi.org/10.1016/j.gca.2017.06.022.

Frisch, M.J., Trucks, G.W., Schlegel, H.B., Scuseria, G.E., Robb, M.A., Cheeseman, J.R., Scalmani, G., Barone, V., Mennucci, B., Petersson, G.A., Nakatsuji, H., Caricato, M., Li, X., Hratchian, H.P., Izmaylov, A.F., Bloino, J., Zheng, G., Sonnenberg, J.L., Hada, M., Ehara, M., Toyota, K., Fukuda, R., Hasegawa, J., Ishida, M., Nakajima, T., Honda, Y., Kitao, O., Nakai, H., Vreven, T., Montgomery Jr., J.A., Peralta, J.E., Ogliaro, F., Bearpark, M., Heyd, J.J., Brothers, E., Kudin, K.N., Staroverov, V.N., Kobayashi, R., Normand, J., Raghavachari, K., Rendell, A., Burant, J.C., Iyengar, S. S., Tomasi, J., Cossi, M., Rega, N., Millam, J.M., Klene, M., Knox, J.E., Cross, J.B., Bakken, V., Adamo, C., Jaramillo, J., Gomperts, R., Stratmann, R.E., Yazyev, O., Austin, A.J., Cammi, R., Pomelli, C., Ochterski, J.W., Martin, R.L., Morokuma, K., Zakrzewski, V.G., Voth, G.A., Salvador, P., Dannenberg, J.J., Dapprich, S., Daniels, A.D., Farkas, Ö., Foresman, J.B., Ortiz, J.V., Cioslowski, J., Fox, D.J., 2009. Gaussian 09.

Graham, T., 1864. On the molecular mobility of gases. Phil. Trans. R. Soc. A 153, 385–405. https://doi.org/10.1098/rstl.1863.0017.

Green, M., Taube, H., 1963. Isotopic fractionation in the OH^-–H_2O exchange reaction. J. Phys. Chem. 67, 1565–1566. https://doi.org/10.1021/j100801a507.

Guo, W., Zhou, C., 2019. Triple oxygen isotope fractionation in the DIC-H_2O-CO_2 system: a numerical framework and its implications. Geochim. Cosmochim. Acta 246, 541–564. https://doi.org/10.1016/j.gca.2018.11.018.

Hayles, J., Gao, C., Cao, X., Liu, Y., Bao, H., 2018. Theoretical calibration of the triple oxygen isotope thermometer. Geochim. Cosmochim. Acta 235, 237–245. https://doi.org/10.1016/j.gca.2018.05.032.

Herwartz, D., 2021. Triple oxygen isotope variations in Earth's crust. Rev. Mineral. Geochem. 86, 291–322. https://doi.org/10.2138/rmg.2021.86.09.

Herwartz, D., Surma, J., Voigt, C., Assonov, S., Staubwasser, M., 2017. Triple oxygen isotope systematics of structurally bonded water in gypsum. Geochim. Cosmochim. Acta 209, 254–266. https://doi.org/10.1016/j.gca.2017.04.026.

Hulston, J.R., Thode, H.G., 1965. Variations in the S^{33}, S^{34}, and S^{36} contents of meteorites and their relation to chemical and nuclear effects. J. Geophys. Res. 70, 3475–3484. https://doi.org/10.1029/JZ070i014p03475.

Hunt, H.R., Taube, H., 1959. The relative acidity of H_2O^{18} and H_2O^{16} coördinated to a tripositive ion. J. Phys. Chem. 63, 124–125. https://doi.org/10.1021/j150571a033.

Huth, T.E., Passey, B.H., Cole, J.E., Lachniet, M.S., McGee, D., Denniston, R.F., Truebe, S., Levin, N.E., 2022. A framework for triple oxygen isotopes in speleothem paleoclimatology. Geochim. Cosmochim. Acta 319, 191–219. https://doi.org/10.1016/j.gca.2021.11.002.

Kim, S.-T., Mucci, A., Taylor, B.E., 2007. Phosphoric acid fractionation factors for calcite and aragonite between 25 and 75 °C: Revisited. Chem. Geol. 246, 135–146. https://doi.org/10.1016/j.chemgeo.2007.08.005.

Luz, B., Barkan, E., 2010. Variations of $^{17}O/^{16}O$ and $^{18}O/^{16}O$ in meteoric waters. Geochim. Cosmochim. Acta 74, 6276–6286. https://doi.org/10.1016/j.gca.2010.08.016.

Matsuhisa, Y., Goldsmith, J.R., Clayton, R.N., 1978. Mechanisms of hydrothermal crystallization of quartz at 250°C and 15 kbar. Geochim. Cosmochim. Acta 42, 173–182. https://doi.org/10.1016/0016-7037(78)90130-8.

McConnaughey, T., 1989a. ^{13}C and ^{18}O isotopic disequilibrium in biological carbonates: II. *In vitro* simulation of kinetic isotope effects. Geochim. Cosmochim. Acta 53, 163–171. https://doi.org/10.1016/0016-7037(89)90283-4.

McConnaughey, T., 1989b. ^{13}C and ^{18}O isotopic disequilibrium in biological carbonates: I. Patterns. Geochim. Cosmochim. Acta 53, 151–162. https://doi.org/10.1016/0016-7037(89)90282-2.

Miller, M.F., 2002. Isotopic fractionation and the quantification of ^{17}O anomalies in the oxygen three-isotope system: an appraisal and geochemical significance. Geochim. Cosmochim. Acta 66, 1881–1889. https://doi.org/10.1016/S0016-7037(02)00832-3.

Pack, A., Herwartz, D., 2014. The triple oxygen isotope composition of the Earth mantle and understanding $\Delta^{17}O$ variations in terrestrial rocks and minerals. Earth Planet. Sci. Lett. 390, 138–145. https://doi.org/10.1016/j.epsl.2014.01.017.

Richet, P., Bottinga, Y., Javoy, M., 1977. A review of hydrogen, carbon, nitrogen, oxygen, sulphur, and chlorine stable isotope fractionation among gaseous molecules. Annu. Rev. Earth Planet. Sci. 5, 65–110. https://doi.org/10.1146/annurev.ea.05.050177.000433.

Sade, Z., Halevy, I., 2017. New constraints on kinetic isotope effects during $CO_{2(aq)}$ hydration and hydroxylation: revisiting theoretical and experimental data. Geochim. Cosmochim. Acta 214, 246–265. https://doi.org/10.1016/j.gca.2017.07.035.

Schauble, E.A., 2004. Applying stable isotope fractionation theory to new systems. Rev. Mineral. Geochem. 55, 65–111. https://doi.org/10.2138/gsrmg.55.1.65.

Schoenemann, S.W., Schauer, A.J., Steig, E.J., 2013. Measurement of SLAP2 and GISP $\delta^{17}O$ and proposed VSMOW-SLAP normalization for $\delta^{17}O$ and $^{17}O_{excess}$. Rapid Commun. Mass Spectrom. 27, 582–590. https://doi.org/10.1002/rcm.6486.

Urey, H.C., 1947. The thermodynamic properties of isotopic substances. J. Chem. Soc. 562–581 https://doi.org/10.1039/JR9470000562.

Wostbrock, J.A.G., Brand, U., Coplen, T.B., Swart, P.K., Carlson, S.J., Brearley, A.J., Sharp, Z.D., 2020a. Calibration of carbonate-water triple oxygen isotope fractionation: seeing through diagenesis in ancient carbonates. Geochim. Cosmochim. Acta 288, 369–388. https://doi.org/10.1016/j.gca.2020.07.045.

Wostbrock, J.A.G., Cano, E.J., Sharp, Z.D., 2020b. An internally consistent triple oxygen isotope calibration of standards for silicates, carbonates and air relative to VSMOW2 and SLAP2. Chem. Geol. 533, 119432 https://doi.org/10.1016/j.chemgeo.2019.119432.

Young, E.D., Galy, A., Nagahara, H., 2002. Kinetic and equilibrium mass-dependent isotope fractionation laws in nature and their geochemical and cosmochemical significance. Geochim. Cosmochim. Acta 66, 1095–1104. https://doi.org/10.1016/s0016-7037(01)00832-8.

Zeebe, R.E., 2020. Oxygen isotope fractionation between water and the aqueous hydroxide ion. Geochim. Cosmochim. Acta 289, 182–195. https://doi.org/10.1016/j.gca.2020.08.025.